

PROCEEDINGS OF SPIE

[SPIDigitalLibrary.org/conference-proceedings-of-spie](https://spiedigitallibrary.org/conference-proceedings-of-spie)

Simulation of CubeSat caliber particle detector “MiRA_ep” response to energetic electrons and protons using GEANT4 package

Jaromir Barylak, Oleksiy V. Dudnik, Tomasz Woźniczak, Volodymyr O. Adamenko, Ruslan V. Antypenko, et al.

Jaromir Barylak, Oleksiy V. Dudnik, Tomasz Woźniczak, Volodymyr O. Adamenko, Ruslan V. Antypenko, Nikita V. Yezerskyi, Mirosław Kowaliński, Igor Y. Lazarev, Agata Zielińska, Janusz Sylwester, Jarosław Bakała, Piotr Podgórski, "Simulation of CubeSat caliber particle detector “MiRA_ep” response to energetic electrons and protons using GEANT4 package," Proc. SPIE 11176, Photonics Applications in Astronomy, Communications, Industry, and High-Energy Physics Experiments 2019, 111763C (6 November 2019); doi: 10.1117/12.2536748

SPIE.

Event: Photonics Applications in Astronomy, Communications, Industry, and High-Energy Physics Experiments 2019, 2019, Wilga, Poland

Simulation of CubeSat caliber particle detector “MiRA_ep” response to energetic electrons and protons using GEANT4 package

Jaromir Barylak^{*a}, Oleksiy V. Dudnik^{b,a}, Tomasz Woźniczak^a, Volodymyr O. Adamenko^c, Ruslan V. Antypenko^c, Nikita V. Yezerskyi^c, Mirosław Kowaliński^a, Igor V. Lazarev^d, Agata Zielińska^a, Janusz Sylwester^a, Jarosław Bakała^a, Piotr Podgórski^a

^aSolar Physics Division of the Space Research Centre of Polish Academy of Sciences, Kopernika str., 11, Wrocław, Poland 51-622; ^bInstitute of Radio Astronomy of National Academy of Sciences of Ukraine, Mystetstv str., 4, Kharkiv, Ukraine 61002, ^cNational Technical University of Ukraine “Igor Sikorsky Kyiv Polytechnic Institute”, Peremohy Ave., 37, Kyiv, Ukraine 03056, ^dInstitute for Scintillation Materials of National Academy of Sciences of Ukraine, Nauki Ave. 60, Kharkiv, Ukraine 61072

ABSTRACT

In recent years, interest in revealing, registering, analyzing and interpretation of the short-term (0.1-1 s) sharp increases in the number of high-energy charged particles at LEO (Low Earth Orbit) has substantially increased. This is due to the profound influence of geomagnetic disturbances on the state of the Van Allen radiation belts, one of the important components of space weather. At the same time, in recent years, principally new technologies have been rapidly developed, both in the area of detection of the elementary charged particles and in construction of space microelectronics. In particular, over the past years, nanosatellites in the CubeSat standard were developed, manufactured and launched into LEO, whose mission was to record and study the characteristics of electron microbursts precipitating from the Earth radiation belts.

Here, we present the concept of a compact instrument developed in the 1U CubeSat standard which is aimed to study the nature of high-energy charged particles microbursts present in the Earth magnetosphere. A functional diagram, a description of the structural modules and the technical characteristics of the miniaturized electron-proton recorder-analyzer MiRA_ep are shown. We have carried out and present the results of computer simulation of the physical processes caused by high-energy electron and proton passage through sensors of the detector head of the MiRA_ep device. The simulation was carried out with the Monte Carlo method using the CERN GEANT4 package. The values of most probable deposited energies were calculated for a wide range of primary electrons and proton energies. This allowed us to make a conclusion about the effective energy ranges of the proposed instrument. The results of these simulations will be used in developing analog and digital signal processing electronic units.

Keywords: Van Allen radiation belts, electrons, protons, CubeSat standard, computer simulation, GEANT4, functional scheme, energy range

1. INTRODUCTION

Detection of the microbursts of high-energy electrons registered at the peripheral edge of the outer electron radiation belt [1], at low latitudes and in the near-equatorial zone [2] is one of the significant achievements in the study of space ionizing environment. Another one is the registration of short-lived radiation belts in the slot between Van Allen inner and outer belts as well as below the inner electron belt [3]. Radiation zones, sporadically being generated in the slot between Van Allen belts, at mid-latitudes, and particle microbursts on the edges of radiation belts are not yet studied sufficiently. Researchers have not yet proposed credible mechanisms for generating the intense electron bursts at middle and low latitudes, which is observed on LEO satellites.

*jbarylak@cbk.pan.wroc.pl; phone 48 71 374-76-85; fax 48 71 372-93-72; www.cbk.pan.wroc.pl

Different kind of space instruments is being developed with a purpose to solve the listed scientific tasks. The researchers plan or have already implemented the miniature satellite devices for high energy elementary charged particles monitoring. Indian scientists and students from the Madras Institute of Technology developed a compact device SPEED for the registration of electrons and protons on board the nanosatellite IITMSAT [4]. This device is aimed to study precipitating charged particles from the Van Allen radiation belts related to seismo-electromagnetic emissions. The silicon PIN and scintillation CsI(Tl) detectors are used as sensors in the RADMON instrument of the Finnish student nanosatellite Aalto-1 [5].

In this paper, we propose own satellite experiment for studies of the nature of microbursts of high-energy charged particles. The experiment will be based on the compact **M**iniaturized **R**egistrant-**A**nalyzer of electrons and protons MiRA_ep. Results of the computer simulation of the physical processes caused by high-energy electron and proton passage through the sensors of the detector head are presented.

2. BRIEF DESCRIPTION OF THE “MIRA_EP” INSTRUMENT

2.1 A structural scheme of the device

The MiRA_ep instrument as a payload of the nanosatellite in a CubeSat format will comprise of three modules: detector head as well as analog and digital units (see Figure 1). Each of the modules is a separate block, which is connected with each other via cables and connectors. The DC/DC voltage converters will be installed in the analog and digital modules, which will provide these modules by necessary voltage levels.

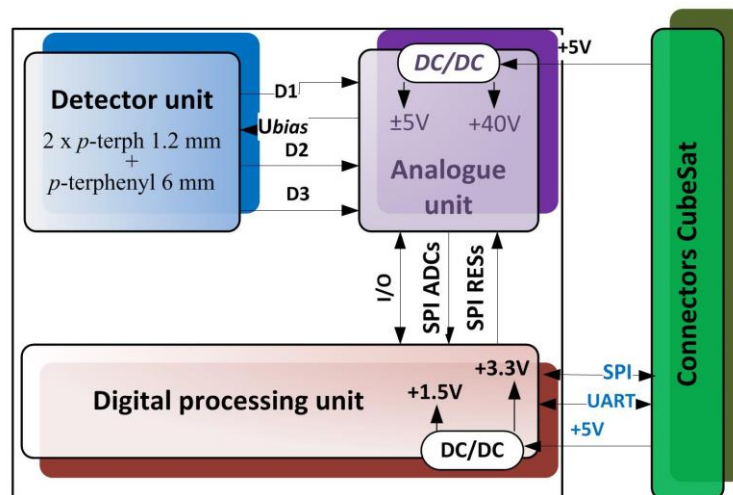


Figure 1. A structural scheme of the **M**iniaturized **R**egistrant-**A**nalyzer of electrons and protons MiRA_ep.

The detector head will consist of two thin scintillation D1 and D3 detectors and one thick scintillation detector D2 of total energy absorption manufactured from the *p*-terphenyl single crystal. The head will also contain a collimator system that will restrict angle of view in two opposite directions. Detectors will be inserted into the mechanical design so that to form a bidirectional telescopic system. A mechanical collimating construction will form the solid angle with cross-cut angle of view of the device $\Delta\theta = 34^\circ$.

The analog module will consist of three spectrometric analog electronic channels: the two identical channels will process and shape analog signals incoming from also identical thin D1 and D3 detectors. The third spectrometric electronic channel will shape the signals incoming from a thick scintillation detector D2.

2.2 Scintillation detectors

The detection and spectrometry of subrelativistic electrons are carried out effectively with the usage of organic scintillators. These materials change particle motion trajectories slightly only due to their small atomic numbers. This leads to the almost full absence of the backscattering of the particles. A low density and effective atomic number of elements composing the organic scintillators make detectors to be less sensitive to the registration of X-rays and gamma-radiation in comparison with the inorganic scintillators. Particularly, authors [6] have shown that the relation of a quantity of gamma-radiation photons to the number of conversion electrons for an energy $E_1=50$ keV made up 11%, and for energy $E_2=300$ keV this value decreased down to 3%. A short decay time ($\sim 3 \times 10^{-8}$ s) of the luminescence in comparison with a longer decay time for inorganic scintillators ($\sim 10^{-6}$ s and more) is an important advantage of organic scintillators. They are also highly transparent to the spectrum of own fluorescence.

The *p*-terphenyl is one of such type of organic scintillators. It has a relatively high melting point ($T = 214^\circ\text{C}$) and a low cost. The absolute value of the light output of this scintillator is 24,950 photons / MeV [7]. The *p*-terphenyl, doped with 1,4-diphenyl-1,3-butadiene we used as a material for sensors manufacturing of the MiRA_ep instrument.

The *p*-terphenyl single crystal with a heightened light yield was grown with the purpose to produce the two thin detectors (ΔE -detectors) and a total energy absorption detector as constituent sensors of the detector head. The amount of 1,4-biphenyl-1,3-butadiene dopant was increased from 0.1 wt % (typical value) to 0.3 wt % [8]. A cylinder of the thickness 7 mm was cut out from the grown ingot at right angles to the growth direction of the single crystal (Figure 2).



Figure 2. An ingot of the *p*-terphenyl single crystal grown by the Bridgman method (a); a cylindrical workpiece of the *p*-terphenyl with the crystallographic axes direction marking, and the *p*-terphenyl single crystal in a parallelogram form after mechanical treatment.

The direction of growth of the *p*-terphenyl single crystal coincides with the *c* axis of the single crystal, so the base of the cylinder matches up with the cleavage plane *ab*. The crystal was oriented along the crystallographic axes *a* and *b* with the usage of red emitting laser in order to determine the direction of further cutting to requested dimensions. Cut pieces of the single crystals have been abraded to the required sizes. Polishing of the samples was carried out using the polishing composition described in [9]. Such special polishing composition provided an improvement of the polished surface quality and increased scintillation and optical characteristics of the detectors due to the enhancement of the light collection coefficient.

The difference in the technical light yield values along the crystallographic lattice axes for the *p*-terphenyl single crystal also has been taken into consideration in detectors manufacturing process. Particularly, in previous works, we showed that the highest technical light yield was detected along the axis *b* of the *p*-terphenyl crystallographic lattice [10, 11, 12, 13], carrying out studies of scintillation properties of a small cube-shaped detector along characteristic axes *a*, *b* and *c*. Figure 3 demonstrates manufactured ΔE -detectors (*a* and *c*) and the detector of total energy absorption (*b*) to be placed inside of the detector head, a design of which is shown in Figure 4.

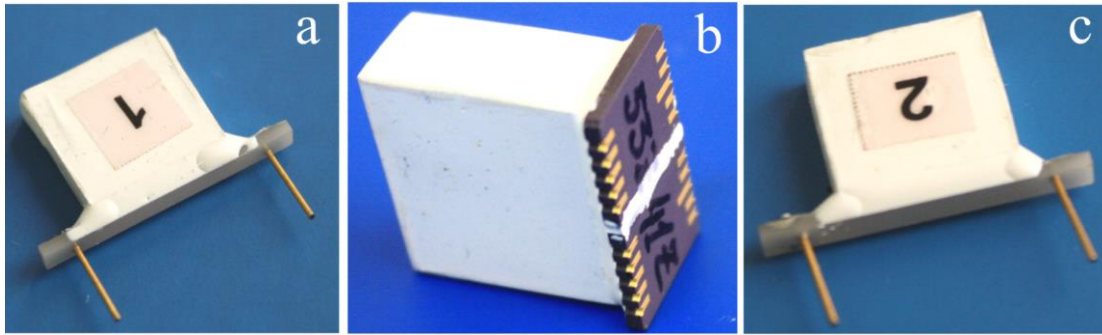


Figure 3. The p -terphenyl scintillation detectors of the MiRA_ep instrument.

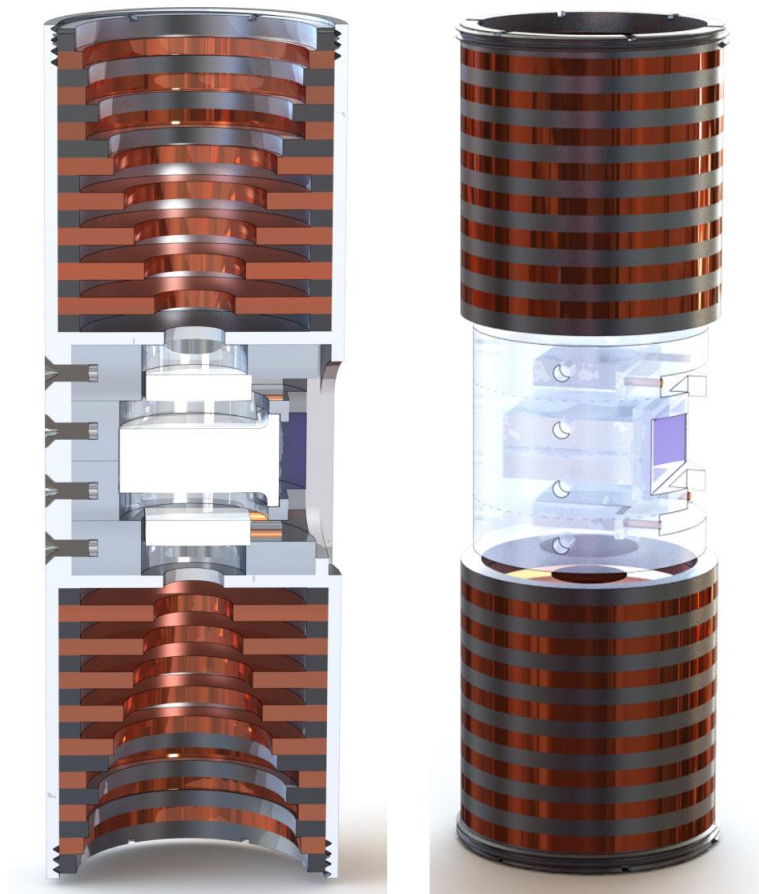


Figure 4. An artistic view of the detector head of the MiRA_ep instrument.

2.3 Specifics of operation logic of the digital processing unit

The structural and functional block-diagrams of the digital signal processing unit are presented in Figures 5 and 6. The three high-speed PulSAR ADCs ($ADC-1$, $ADC-2$, $ADC-3$) with pseudo differential inputs and serial output have been chosen due to the serial differential exit of the analog part as well as based on the high data transmission speed (1 MSPS and higher).

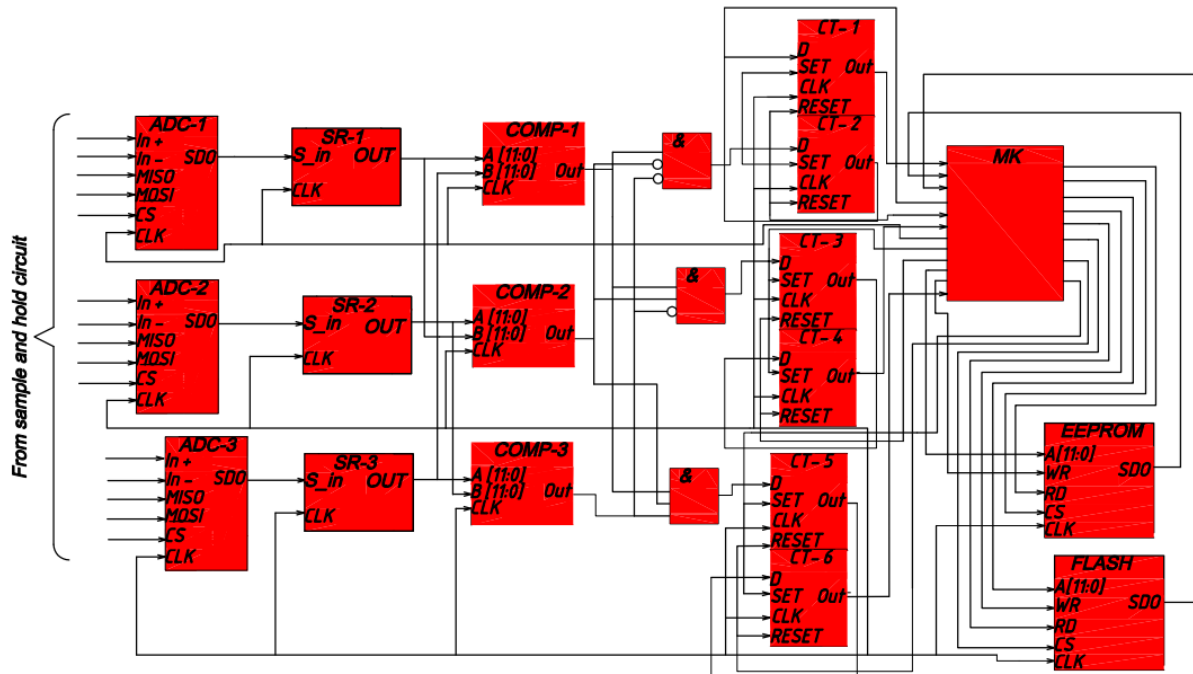


Figure 5. A structural diagram of the digital signal processing unit. Explanations are given in the text.

To compare the value of deposited energies represented in the ADC codes it is necessary to convert the serial data with a shift register (*SR*) and compare it on digital comparators (*DC-1*, *DC-2*, *DC-3*). The solver (*S*) is designed on three constituent logical elements. It provides a work of the increment counter (*CT-1*, ..., *CT-6*) for each type of particles. Existence of two counters per each channel is being required to provide a reduction of the rewrite cycles [14]. The two different types of memory (*EEPROM*, *FLASH*) are intended for greater reliability of data storage. The microcontroller unit (*MCU*) provides general control, clocking and write / read data from the memory.

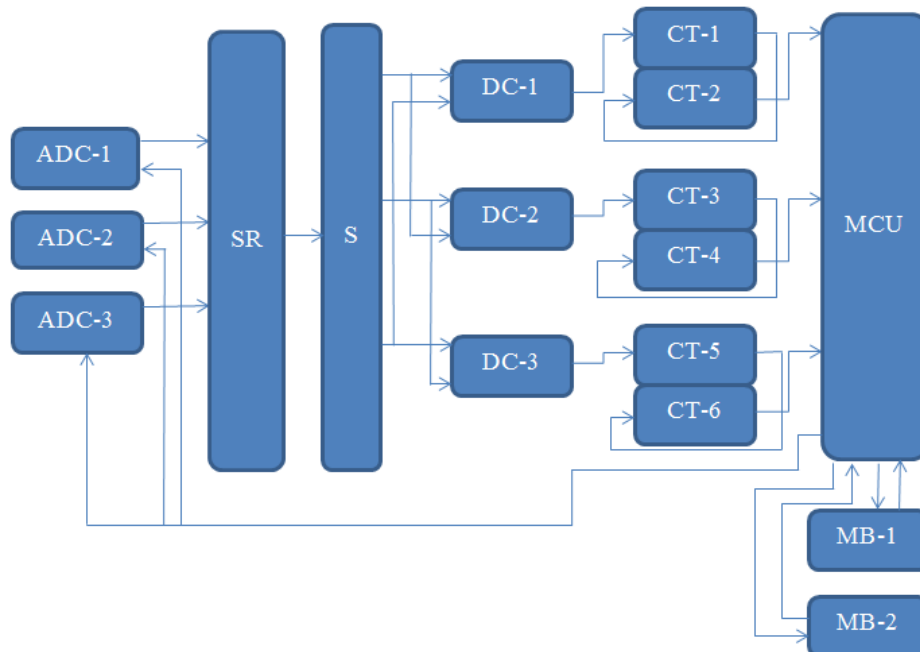


Figure 6. Functional block diagram of the digital signal processing unit.

3. SIMULATION DESCRIPTION

3.1 Geant4 toolkit

Into Monte Carlo simulation we used Geant4 [15] toolkit basically developed for high energy physics. Now, this tool continues to be the simulation engine of high energy physics experiments like LHC (Large Hadron Collider). ESA and NASA have used Geant4 in the design of spacecraft instruments [16], its background [17, 18, 19] and design of the radiation shields. Additionally, this tool is used in medical physics, biochemistry, and material science. Such a wide spread of usage is possible because there are a lot of physic models available which can be freely selected. These physical models describe the interaction between particles and matter in a broad range of energies from 250 eV (10 eV for electrons) to some TeV.

3.2 Simulation description

We recreated the whole geometry of the detector (Figure 7): aluminum filter (thickness: 100 μm), collimators and p-terphenyl detectors. To obtain the response of detectors, we used planar source covering the whole entrance window of the instrument. Particles of the source fell at the right angle and their distribution on the entrance window was assumed uniform. The number of incident particles was selected to be 10^6 . We used G4EmLowEPPysics physics list, which consists of all electro-magnetic processes optimized for low energy. Detector effects were not included.

We made two kinds of simulations for two types of particles: electrons and protons. In the first one, we used entire uniform spectrum of particles in the range: for electrons from 20 keV to 10 MeV and for protons from 1 MeV to 100 MeV. The second type of source was monoenergetic injector of electrons. Information on deposited energy in each detector after simulation of each particle was collected.

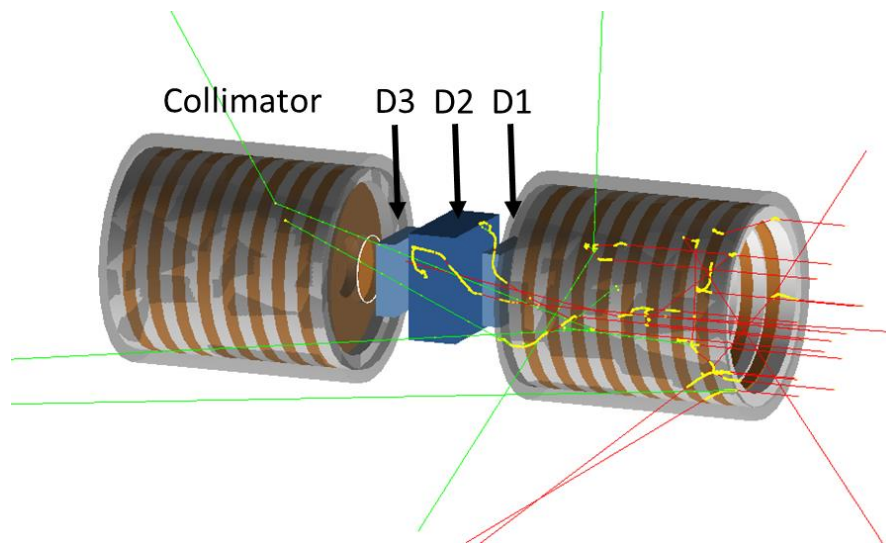


Figure 7. Geant4 simulation of the instrument. By red color electron tracks are presented, by green color the photon's tracks.

4. RESULTS OF SIMULATION

4.1 The detection capability of the instrument.

Results of modeling of the detection capability is shown in Figure 8. Black and blue dots correspond to simulated electrons measured in D1 and D2 detectors respectively. The same red and green dots correspond to counts of protons. The first detector measure electrons (black dots) up to 1.5 MeV, but it becomes transparent above 1 MeV. Most of the electrons with energies lower than 200 keV are stopped by the aluminum filter. For electrons with energy above 4 MeV, the second detector D2 becomes transparent.

Measurements of protons start above 3 MeV and will continue in the D1 detector until 18 MeV. The large detector can stop protons with energy below 38 MeV. Above this energy, protons leave D2 detector and part of them can reach the third thin D3 detector, but such types of events will be removed from data collection and processing

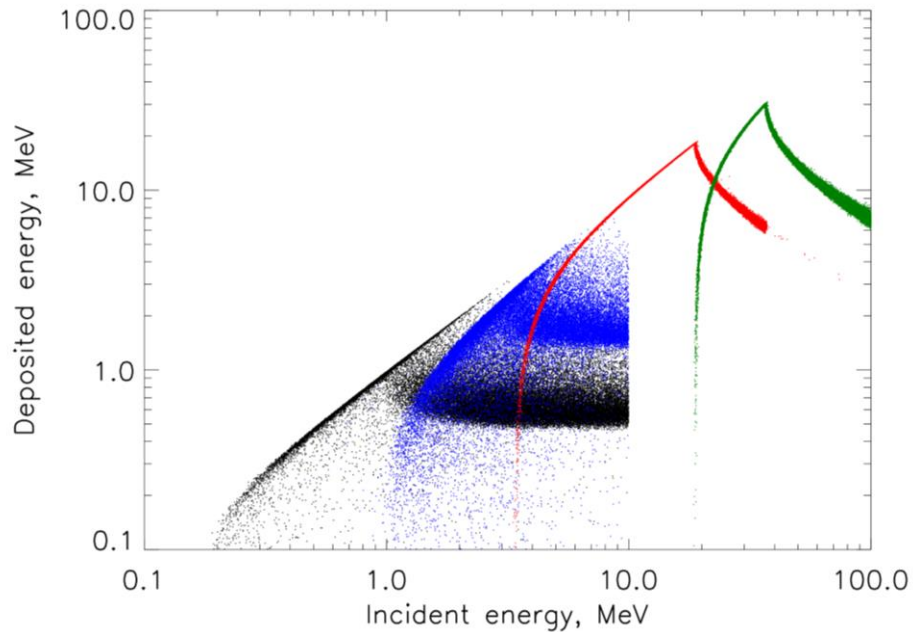


Figure 8. Counts of MiRA_ep detectors. Black dots represent counts of electrons in D1 detector, blue one – electrons in D2 detector. Counts of protons are presenting by red (first detector) and green (second detectors) dots.

Figure 8 and 9 demonstrate spectra obtained with detectors being irradiated by monoenergetic electrons and protons respectively. In D2, peaks are shifted to lower energies because particles deposited part of their energy in D1 detector.

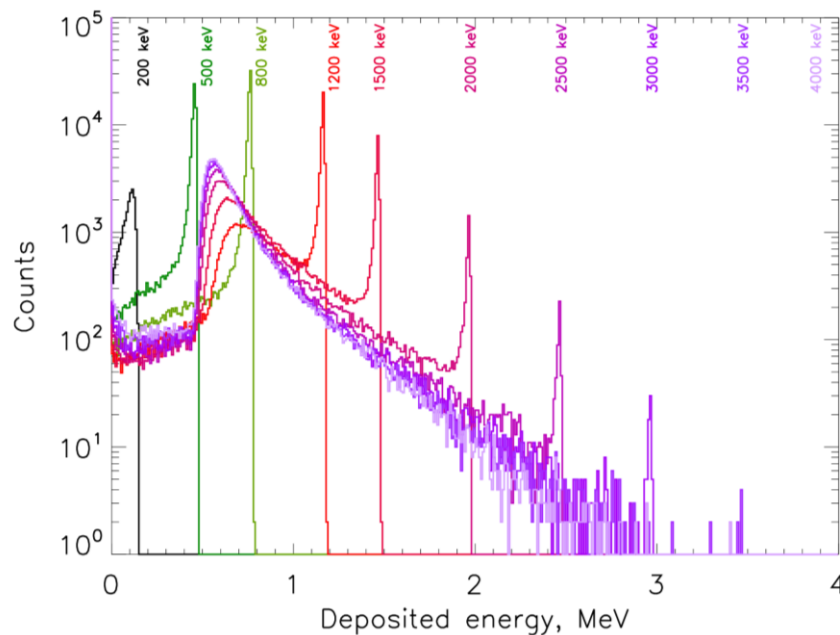


Figure 9. D1 response to passing monoenergetic electrons. The energy of electrons is color coded.

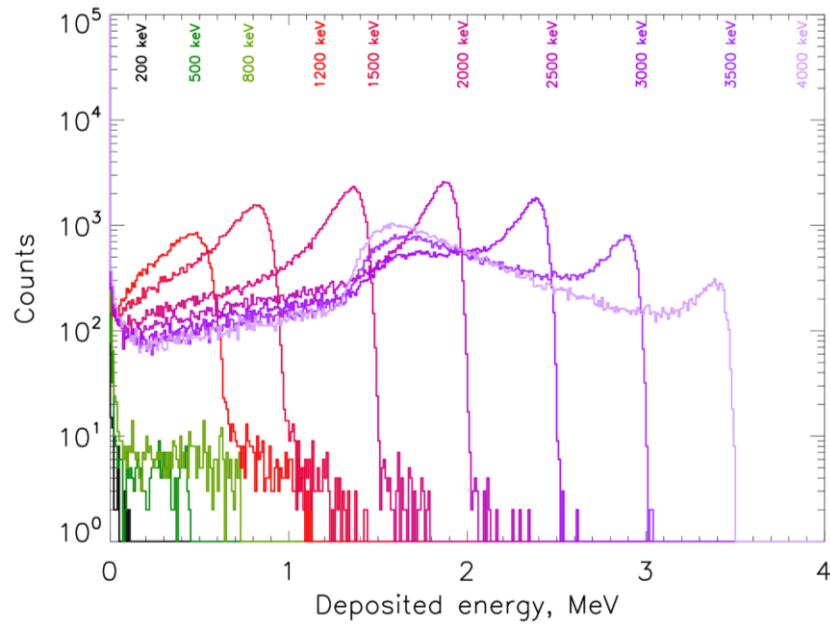


Figure 10. D2 detector response to passing monoenergetic electrons. The energy of electrons is also color coded.

4.2 The method of recognizing the type of particles

To recognize the type of particle we need to know a dependence of deposited energies in the first thin D1 detector on the deposited energies in the second thick D2 detector. In figure 11 there are shown events registered in both detectors, by black dots the electrons, by blue dots the protons. It is clearly seen that the protons deposit much more energy to the p-terphenyl detectors comparatively with electrons in case of workable logic $D1D2\bar{D3}$ of the MiRA_ep instrument so that electrons can be distinguished from protons very well.

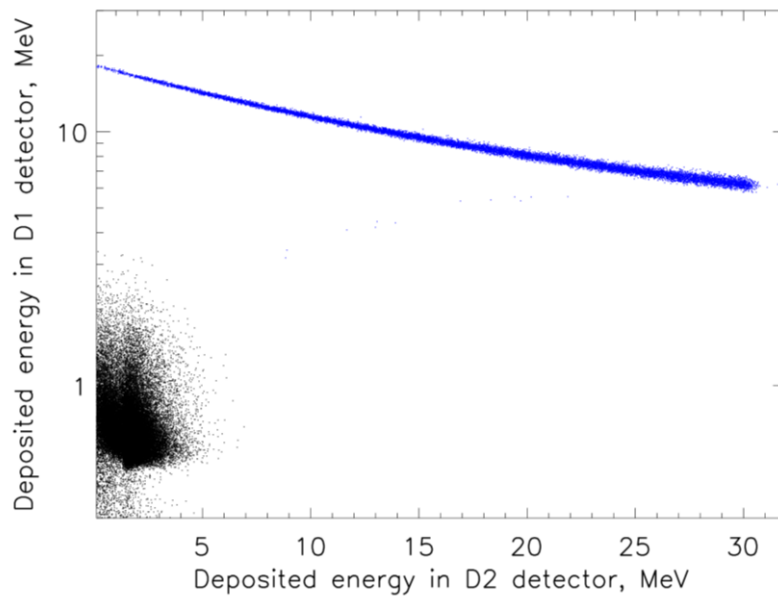


Figure 11. Deposited energy in D1 detector vs deposited energy in D2 detector. Black dots presented the electrons, blue dots protons.

5. CONCLUSION

Further investigations of particle flux variations filling the Van Allen Earth radiation belts, monitoring, and understanding of the nature and fine structure of the short-term electron microbursts is proposed with the usage of the miniaturized registrant-analyzer MiRA_ep in a CubeSat format. The distinctive features of this small-sized instrument are the application of organic scintillator on the base of *p*-terphenyl single crystal and registering of particles from the two mutually opposite directions. The last one will allow studying the degree of anisotropy of microbursts.

Monte-Carlo simulation with the usage of GEANT4 package allowed estimating energy ranges of electrons and protons to be detected by the telescopic system based on organic scintillators. Incident electrons will be measured from $E_{emin} \approx 200$ keV up to energies of $E_{emax} \leq 4$ MeV, and incident protons can be registered from $E_{pmin} \approx 3.5$ MeV up to energy $E_{pmax} \leq 40$ MeV. Computer simulation of both detectors' responses demonstrated also confident way to distinguish between electron and protons.

We are planning to add detectors effects [20] during the next stages of our work in the modeling of the MiRA_ep instrument

Acknowledgement

This work was supported by the Interdepartmental Council for Instrument Engineering of the National Academy of Sciences of Ukraine Grant No. 2.31.16 and Polish National Science Centre grant number UMO-2015/19/B/ST9/02826.

REFERENCES

- [1] Nakamura, R., Isowa, M., Kamide, Y., Baker, D. N., Blake, J. B., and Looper, M., "SAMPEX observations of precipitation bursts in the outer radiation belt", *J Geophys. Res. Space Phys.*, 105(A7), 15875-15885 (2000).
- [2] Nagata, K., Kohno, T., Murakami, H., Nakamoto, A., Hasebe, N., Kikuchi, J., et al., "Electron (0.19-3.2 MeV) and proton (0.58-35 MeV) precipitations observed by ONZORA satellite at low latitude zones $L=1.6-1.8$," *Planet. Space Sci.*, 36(6), 591-606 (1988).
- [3] Hudson, M. K., Kress, B. T., Mueller, H.-R., Zastrow, J. A., and Blake, J. B., "Relationship of the Van Allen radiation belts to solar wind drivers", *J Atmos. Sol.-Terr. Phys.*, 70(5), 708-729 (2008).
- [4] Surya Teja, S. S., Subramanyan, V., Elangovan, R., Reddy, L. M., Ramachandran, D., Harshavardhan. M., et al., "Design of Nuclear Instrumentation for Space-based Proton-Electron Energy Detector (SPEED)", *Proc. Intern. Conf. on Space Science and Communication (IconSpace)*, Kuala Lumpur, Malaysia, 10-12 August 2015, 181-186 (2015).
- [5] Peltonen, J., Hedman, H-P., Ilmanen, A., Lindroos, M., Maattanen, M., Pesonen, J., et. al., "Electronics for the RADMON instrument on the Aalto-1 student satellite", *Proc. 10th European Workshop on Microelectronics Education (EWME)*, Tallinn, Estonia, 14-16 May 2014, 161-166 (2014).
- [6] Angelone, M., Battistoni, G., Bellini, F., Bocci, V., Collamati., F., De Lucia, E., Faccini, R., Ferroni, F., Fiore, S., Marafini, M., Materazzo, D., Mattei, I., Morganti, S., Patera, V., Piersanti, L., Pillon, M., Recchia, L., Russomando, A., Sarti, A., Sciubba, A., Solfaroli Camillocci, E., and Voena, C., "Properties of para-Terphenyl as a Detector for α , β , and γ Radiation", *IEEE Trans. Nucl. Sci.*, 61(3), 1483 - 1486 (2014).
- [7] Galunov, N. Z., Tarasenko, O. A., and Tarasov, V. A., "Determination of light yield of organic scintillators", *Funct. Mater.*, 20(3), 304-309 (2013).
- [8] Galunov, N. Z., Lazarev, I. V., Martynenko, E. V., Vashchenko, V. V., and Vashchenko, E.V., "Distribution coefficient of 1,4-diphenyl-1,3-butadiene in p-terphenyl single crystal and its influence on scintillation crystal light output", *Mol. Cryst. Liq. Cryst.*, 616(1), 176-186 (2015).
- [9] Tarasov, V. O., Andryushchenko, L. A., Dudnik, O. V., and Rybka, E. A., "Influence of surface treatment conditions for organic crystalline scintillators on their scintillation characteristics", *Funct. Mater.*, 25(1), 144-150 (2018).

- [10] Dudnik, O. V., Lazarev, I. V., Kurbatov, E. V., Kowaliński, M., Podgorski, P., and Ścisłowski, D., “Advisability of the axes orientation in *p*-terphenyl crystal of scintillation detector of the charged particle monitor in ChemiX solar X-ray spectrophotometer (in Russian)”, *Space Sci. Technol.*, 24(3), 33-39 (2018).
- [11] Dudnik, O. V., Kurbatov, E. V., Lazarev, I. V., Sylwester, J., Kowaliński, M., and Gburek, S., “A method to pile up the technical light output of organic scintillator in BPM particle detector of the ChemiX solar X-ray spectrophotometer”, *Proc. 17th Ukrainian conference on space research, Odesa, Ukraine*, 75 (2018).
- [12] Dudnik, O. V., Lazarev, I. V., Sylwester, J., Siarkowski, M., and Kowaliński, M., “Feasibility of a usage of small-sized *p*-terphenyl scintillators with oriented crystalline axes in space measurements of high-energy charge radiation”, *Abstracts 42nd COSPAR Scientific Assembly, Pasadena, CA, USA, 1954-1955 July 2018*.
- [13] Lazarev, I. V., Dudnik, O. V., Kowaliński, M., and Podgorski, P., “Evidence of the light yield anisotropy for small *p*-terphenyl single crystal”, *Abstracts 6th Intern. Conf. “Engineering of scintillation materials and radiation technologies (ISMART 2018)”*, Minsk, Belarus, 66-67 (2018).
- [14] Tocci, R. J., Widmer, N. S., and Moss, G. L., [*Digital Systems. Principles and Applications*], Pearson Prentice Hall, New Jersey Columbus, Ohio, USA, 970p, (2007).
- [15] Allison, J., Amako, K., Apostolakis, J., et. al. *Recent Developments in Geant4. Nucl. Instrum. Meth. A* 835, 186-225 (2016).
- [16] Barylak, J., Podgórski P., Mrozek T., et al., “Geant4 simulations of detector response matrix for Caliste-SO”, *Proc. SPIE 9290, 929037* (2014).
- [17] A. Gorgolewski, J. Barylak, M. Stęślicki, Ż. Szaforz, and J. Bąkała, “Solpex x-ray polarimeter detector luminescence background calculated using geant4 simulation software”, *Proc. SPIE 10031, 100313V* (2016).
- [18] Barylak, J., Barylak, A., Mrozek T., et al., “Investigation of cosmic ray and solar energetic particle background of STIX using GEANT4 simulation”, *Proc. SPIE 10808, 1080848* (2018).
- [19] Makowski, A., Barylak, J., Stęślicki, M., et al., “Geant4-based simulations of the x-ray luminescence background in the rotating drum spectrometer/SOLPEX”, *Proc. SPIE 10808, 1080846* (2018).
- [20] Barylak, J., Barylak, A., Mrozek T., et al., “Simulation of charge sharing in the Caliste-SO detector”, *Nucl. Instrum. Meth. A* 903, 234-240 (2018).